A new GIS landscape classification method for rain/snow temperature thresholds in surface based models

James M. Feiccabrino and Laurie D. Grigg

ABSTRACT

Landscape air temperature thresholds (T_A) and percent misclassified precipitation (error) for 12 years of meteorological observations from 40 stations across the Scandinavian Peninsula were derived and compared using both manual and geographic information system (GIS) landscape classification methods. Dew-point, wet-bulb, and wet bulb 0.5 were also tested. Both classification methods used the following west to east landscape categories: windward (WW) ocean, coast, fjord, hill, and mountain in Norway; and leeward (LW) mountain, hill, rolling terrain, and coast in Sweden. GIS landscape classification has the advantages of automating the classification process and increasing objectivity. The GIS classification was based on station location (LW or WW) relative to the Scandinavian mountain range, and the % water or range of elevation change within 15 km. The GIS and manual method had the same T_A for 20 stations, and similar total reduction in error (2.29 to 2.17% respectively) when compared to country T_A. Therefore, automated GIS landscape classification can be used to decrease error from common country or global scale T_A. Wet-bulb temperature thresholds for GIS landscapes resulted in a greater reduction in error (8.26%) compared to air (2.29%), and dew-point (−16.67%) thresholds. However, finding stations reporting relative humidity or wet-bulb temperature may limit its widespread use.

Key words | geographic landscape, hydrology, precipitation phase, snow, snow model, temperature threshold

James M. Feiccabrino (corresponding author)
Water Resources Engineering,
Lund University,
Lund S-221 00,
Sweden
E-mail: *james.feiccabrino@googlemail.com*

James M. Feiccabrino
Laurie D. Grigg
Department of Earth and Environmental Sciences,
Norwich University,
158 Harmon Drive,
Northfield,
Vermont 05663,
USA

INTRODUCTION

Precipitation falling as rain or snow can affect many different aspects of life such as transportation safety on roads, strength or thickness of sea ice (Lundberg & Feiccabrino 2009), runoff in rivers, animal migration patterns (Stenseth *et al.* 2002), or water storage in reservoirs for electricity production, drinking, or recreation. Surface based models for these purposes use a precipitation phase determination scheme (PPDS) to assign precipitation to a liquid (rain) or solid (snow) phase. Many PPDS apply a surface air temperature threshold (T_A) (e.g. USACE 1956), surface dew point temperature threshold (T_D) (e.g. Marks *et al.* 2013), or a surface wet bulb temperature threshold (T_W) (e.g. Matsuo *et al.* 1981).

A PPDS scheme often uses either: (1) a single temperature threshold (T_{RS}) where all precipitation events occurring in temperatures equal to or colder than a T_{RS} are classified as snow, while all events occurring in warmer temperatures are classified as rain; or (2) a dual temperature threshold scheme using a rain (T_R) and snow (T_S) temperature threshold with all precipitation occurring in temperatures equal to or colder than T_S classified as snow, all events occurring in temperatures equal to and warmer than T_R classified as rain, and for precipitation in temperatures between T_S and T_R a decreasing snow fraction (SF) from $T_S = 100\%$ to $T_R = 0\%$ is used to assign the precipitation phase. The advantage of a dual threshold scheme is that it

doi: 10.2166/nh.2016.055

can account for sleet occurring in temperatures near a T_{RS}, however in some areas sleet is rarely reported. For PPDS purposes, the T_{RS} or T_S and T_R are set to the temperature value/s resulting in the least amount of misclassified precipitation. These threshold values are often applied over large areas irrespective of terrain, ocean, or seasonal influences on different landscapes. These and other methods, along with meteorological reasoning for their use, are reviewed in Feiccabrino *et al.* (2015).

Surface based PPDS methods do not account for microphysical processes, e.g. evaporation, sublimation, freezing and melting (Thériault & Stewart 2010), which are very calculation intensive, and important for assigning a precipitation phase in atmospheric models. The calculations of microphysical processes require detailed lower atmospheric measurements not often brought into surface (hydrological) models (Harder & Pomeroy 2013). Instead, surface models rely on the assumption of constant atmospheric conditions, such as a set decrease in air temperature with height (e.g. the CHRM model using −7.5 °C/km lapse rate) (Fang *et al.* 2013).

Assuming constant atmospheric conditions over a large area with varying landscapes is not ideal when, for example, a snowpack (open water) conductively cools (warms) near surface air. The atmospheric depth to which land or ocean temperatures have an effect is generally restricted to a couple hundred meters, and this depth can increase or decrease depending on the amount of time an air-mass is over the cooling (heating) source, wind speeds, or other factors. Terrain effects, for example orographically enhanced precipitation, will increase the depth of the atmosphere required to melt falling snow (the melting layer) toward the ground due to increased heat energy required to melt the additional snow. This results in a lowering of the 0 °C isotherm and snow elevations compared to upwind locations (Minder *et al.* 2011). Therefore, increasing the precipitation rate would cause changes from the surface model assumption of constant atmospheric conditions by lowering cloud layers, snow elevations, and the 0 °C isotherm. The degree to which orographic enhancement occurs is dependent on the geometry of the terrain, and melting layer properties (Minder *et al.* 2011), for example, relative humidity (RH). On the leeside of mountains, air descends drier, and warms at or near the dry adiabatic lapse rate (9.8 °C/km) causing another change from normal atmospheric conditions. These terrain effects are known to occur on the individual to hill-slope scale.

Dai (2008), in a global study, found a warm bias of +0.7 °C for T_A over ocean regions (1.9 °C) compared to land regions (1.2 °C). The warm bias over oceans is most likely caused by open water transferring heat to the near surface atmosphere. The added surface warmth increases atmospheric instability (Ólafsson & Haraldsdóttir 2003), which by definition increases the environmental lapse rate, or actual decrease in air temperature with height, compared to the model assumed constant lapse rate. This decreases the depth of an atmospheric warm layer from the expected depth, thus increasing the chance of snow not fully melting before reaching the ground at a given surface air temperature. Stewart (1992) observed that precipitation phase transition often occurred near the coast, supporting the idea of ocean heat affecting lower atmospheric air temperatures which affects the precipitation phase in near coastal locations.

Topography and warm ocean temperatures are therefore known to affect atmospheric conditions above individual locations which should result in different T_A values. However, it is not known if terrain effects can be projected to larger geographical landscapes such as the leeward (LW) side of a mountain range rather than being restricted to the individual hill-slope scale. If station T_A values within a geographical landscape are found to be similar, and differ from values in other landscapes, then geographical regions (countries) could be broken into sub-regions based on landscape categorization to reduce misclassified precipitation error.

This study has two main goals: (1) present a landscape classification technique using geographic information system (GIS) to (a) automate geographic landscape classification, (b) decrease the subjectivity from manual classification found in the earlier conference paper by Feiccabrino (2015), and (c) determine if changes in T_A values for landscape (sub-regional) can be used to decrease error without downscaling to the individual hill-slope scale; and (2) using the same weather stations as the earlier paper, decrease the temperature resolution from 0.5 to 0.1 °C for a comparison of both (a) the misclassified precipitation percentage resulting from PPDS schemes using T_A, T_D, and T_W

and (b) the misclassified precipitation as a result of manual and automated landscape classification.

STUDY AREA

This study is conducted using 40 weather stations; four Norwegian Sea, 16 Norwegian, and 20 Swedish (Table 1); on the Scandinavian Peninsula (Figure 1). The Scandinavian Peninsula is bisected by the Scandinavian Mountain range running SSW to NNE on the Swedish–Norwegian border. Predominant atmospheric winds are from the west and much of the weather impacting the area passes over the Atlantic Ocean and Norwegian Sea before reaching the peninsula. The orientation of the mountain range has two main affects: (1) it causes orographic enhancement on the windward (WW) Norwegian side and down-sloping drying effects on the LW Swedish side of the peninsula; and (2) it can deflect storms NW along the mountains rather than passing west over the mountains.

The weather data are free and publicly available from the Swedish Meteorological and Hydrological Institute (SMHI 2016) and the Norwegian Meteorological Institute (NMI 2016) websites. A description of the data and further station information are found in Feiccabrino (2015). In Feiccabrino (2015), the weather stations were manually assigned to the geographic landscapes; WW ocean, WW coast, WW fjords, WW hills, and WW mountain (valleys) in Norway, and LW mountain (valleys), LW hills, LW rolling, and LW Coast in Sweden. The 2015 study found that using different T_A values for geographic landscapes is a viable option for decreasing misclassified precipitation error in regional studies. It also found T_W to be 0.5 °C in all landscapes (at a 0.5 °C scale), which resulted in less misclassified precipitation than T_D and T_A for eight of nine landscapes. However, dew point, wet-bulb, and RH measurements are much rarer than surface air temperature at hydrological and meteorological sites (e.g. Kane & Stuefer 2015). Therefore it is important to find techniques to decrease misclassified precipitation using surface air temperature, a commonly reported value.

The Scandinavian weather stations have 25–56% winter (October–May) precipitation occurring in surface air temperatures of −3 to 5 °C (Figure 2 and Table 1), a temperature range over which snow and/or rain can occur. Within this air temperature range, there is a high percentage of misclassified precipitation (7–25% in Table 1) for T_A values applied over a regional (country) scale without regard for topography or other local effects.

An initial test applying slight modifications to Dai's (2008) method with different landscape T_A for WW ocean, WW coast, WW fjords, inland, and LW coast stations was found to decrease error from country values (Table 1 and Figure 2). However, better landscape definitions could be used to further decrease misclassified precipitation, especially for inland areas.

METHODS

Geographic coordinates and associated tabular data for each meteorological station were imported into ArcGIS (version 10.2.1) and initially displayed using the WGS 1984 geographic coordinate system. In order to perform spatial analysis, the data were reprojected in a UTM projected coordinate system (ETRS 1989 – TM32). Elevation/hillshade and slope base maps were created using a European digital elevation model (GTOP30) with a 30-arc second (ca. 1 km) resolution. This layer was produced by the USGS EROS Data Center (USGS 1996) and was obtained through ArcGIS online. ArcGIS was used to classify the stations based on landscape features and also to produce a series of maps that highlight the spatial distribution of the results.

The classification of meteorological stations using ArcGIS involved three sets of landscape-based parameters. The first parameter in the classification was used to approximate the water (ocean) or land influence on a weather station. Ice-free water in the winter would normally be a surface based heat source that affects temperature thresholds. Buffer zones of 15 km were created surrounding each station and then intersected with the land outline for Norway and Sweden. The area of land contained within each of the intersected buffer zones was quantified using the calculate geometry function. The following categories were established based on these results: <10% land = ocean; 10–60% land = coast; 60–90% land = fjord (inlet);

Table 1 | Norwegian Sea, Norwegian, and Swedish weather stations names, assigned station numbers, country and adjusted Dai (2008) classification with T_A and percentage of misclassified precipitation as a result of the classification T_A, and the total sample size (with percentage of all precipitation observations between October and May having an air temperature of −3 to 5 °C)

Station name	Station #	Country class	Country T_A	% Misc precip	Dai adj. class	Dai adj. T_A	% Misc precip	Precip sample size
Norwegian sea ocean platforms								**2,368 (34%)**
Ormen Lange	1	Sea	1.8	13.04	Sea	1.8	13.04	93 (28%)
Draugen	2	Sea	1.8	25.18	Sea	1.8	25.18	414 (31%)
Heidrun	3	Sea	1.8	15.43	Sea	1.8	15.43	1,177 (35%)
Norne	4	Sea	1.8	14.93	Sea	1.8	14.93	684 (35%)
Norwegian stations (WW)								**14,073**
Buholmråsa Fyr	5	Norway	1.1	17.68	Sea coast	1.7	16.92	264 (25%)
Nordøyan Fyr	6	Norway	1.1	16.52	Sea coast	1.7	15.75	909 (38%)
Sklinna Fyr	7	Norway	1.1	14.17	Sea	1.8	14.95	516 (45%)
Myken	8	Norway	1.1	13.97	Sea	1.8	13.19	1,150 (38%)
Hjelvik-Myrbø	9	Norway	1.1	18.60	Fjord	1.0	18.27	302 (40%)
Tingvoll-Hanem	10	Norway	1.1	9.13	Fjord	1.0	9.03	970 (45%)
Trondheim-Voll	11	Norway	1.1	13.33	Fjord	1.0	12.96	271 (48%)
Finnøy Hamarøy	12	Norway	1.1	8.60	Fjord	1.0	8.74	693 (43%)
Selbu-Stubbe	13	Norway	1.1	12.94	Inland	1.3	13.44	801 (45%)
Verdal-Reppe	14	Norway	1.1	12.69	Inland	1.3	12.50	1,593 (42%)
Høylandet-Drageidet	15	Norway	1.1	17.26	Inland	1.3	18.37	815 (51%)
Bardufoss	16	Norway	1.1	11.90	Inland	1.3	12.21	1,929 (46%)
Råros Lufthavn	17	Norway	1.1	15.84	Inland	1.3	15.03	623 (39%)
Nordli – Holand	18	Norway	1.1	10.79	Inland	1.3	10.45	1,771 (48%)
Fiplingvatn	19	Norway	1.1	15.49	Inland	1.3	15.15	1,153 (56%)
Saltdal	20	Norway	1.1	11.67	Inland	1.3	8.94	331 (38%)
Swedish stations (LW)								**38,050**
Korsvattnet	21	Sweden	1.3	7.28	Inland	1.3	7.28	3,561 (36%)
Gäddede	22	Sweden	1.3	15.25	Inland	1.3	15.25	581 (35%)
Gielas	23	Sweden	1.3	8.25	Inland	1.3	8.25	2,326 (32%)
Mierkenis	24	Sweden	1.3	9.57	Inland	1.3	9.57	2,756 (29%)
Hemavan	25	Sweden	1.3	10.88	Inland	1.3	10.88	762 (36%)
Föllinge	26	Sweden	1.3	9.72	Inland	1.3	9.72	1,784 (31%)
Hallhåxåsen	27	Sweden	1.3	8.00	Inland	1.3	8.00	1,891 (30%)
Hoting	28	Sweden	1.3	7.06	Inland	1.3	7.06	1,959 (32%)
Gubbhögen	29	Sweden	1.3	8.80	Inland	1.3	8.80	1,992 (31%)
Vilhelmina	30	Sweden	1.3	10.47	Inland	1.3	10.47	1,780 (28%)
Torpshammar	31	Sweden	1.3	10.85	Inland	1.3	10.85	1,796 (35%)
Krångede	32	Sweden	1.3	10.97	Inland	1.3	10.97	2,115 (33%)
Hemling	33	Sweden	1.3	9.04	Inland	1.3	9.04	2,118 (35%)
Fredrika	34	Sweden	1.3	6.78	Inland	1.3	6.78	2,055 (31%)

(*continued*)

Table 1 | continued

Station name	Station #	Country class	Country T_A	% Misc precip	Dai adj. class	Dai adj. T_A	% Misc precip	Precip sample size
Åsele	35	Sweden	1.3	8.44	Inland	1.3	8.44	1,924 (31%)
Kuggören	36	Sweden	1.3	11.15	Coast	1.1	11.37	1,860 (44%)
Brämön	37	Sweden	1.3	10.90	Coast	1.1	11.51	1,945 (44%)
Lungö	38	Sweden	1.3	12.85	Coast	1.1	11.66	1,950 (43%)
Järnäsklubb	39	Sweden	1.3	11.46	Coast	1.1	11.22	2,063 (42%)
Holmön	40	Sweden	1.3	12.08	Coast	1.1	9.54	832 (42%)

>90% land = land (Table 2). These numbers were chosen for their ability to separate the near coastal stations into distinct landscapes with different relative influences of land and ocean. Some smaller islands off the main shore were categorized as ocean stations which could be separated out if another landscape category was added, or the 10% land requirement for coast was decreased.

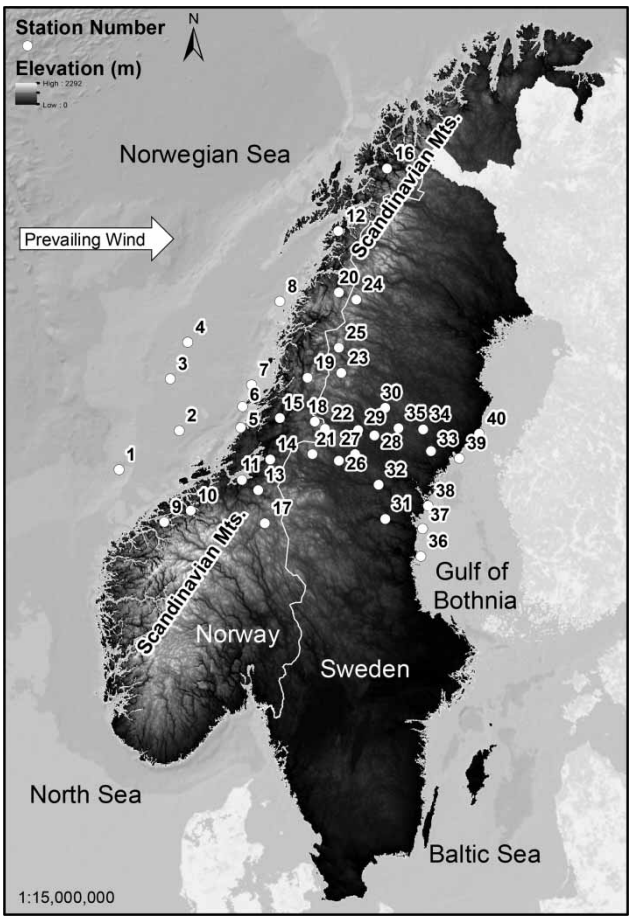

Figure 1 | Study area with station locations and prevailing atmospheric winds.

The land sites were further categorized based on the range of elevation that fell within the 15 km buffer zones. This relief value should indicate the amount of orographic enhancement (Minder *et al.* 2011) or down-sloping (LW) influence on lower atmospheric conditions over an area, therefore providing a reasonable reflection of terrain affects at a higher spatial resolution than the regional scale without having to consider wind datum or more detailed topographic data. The process of calculating the relief value involved extracting the digital elevation model (DEM) that fell within the buffer zones and then converting the extracted DEM into a vector (polygon) feature class. The polygon data were then summarized by station number under the fields of maximum and minimum values. A new table was created during the summarization and the range (max–min elevations) was then calculated for each site buffer using the field calculator. Finally, the new table with range was joined to the original buffer layer. Now each site could be categorized by the range of elevation within each buffer zone. The following classifications were made based on these data: range of 1,500–1,000 m = mountain; range of 1,000–500 m = hill; range of 500–0 m = rolling (Table 2). The values for these classifications were chosen to be both objective with a range of 500 m each, and representative of the amount of relief in the area. The values can be expanded or retracted depending on the topography of a study area, or have extra categories added.

The third and final parameter used in the classification was WW versus LW based on the prevailing direction of westerly flow and the location of the Scandinavian Mountains.

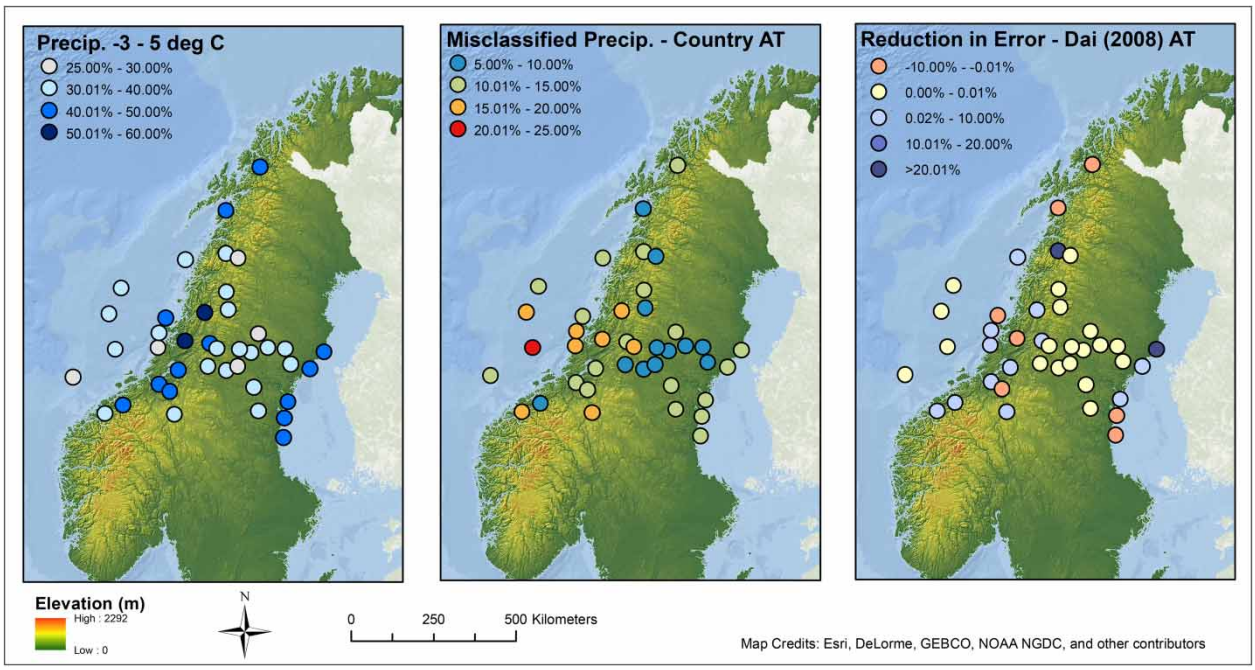

Figure 2 | Charts from left to right depict; % of winter precipitation between −3 and 5 °C, % misclassified precipitation for observations between −3 and 5 °C using country (Norwegian Sea, Norway, and Sweden) T_A values, and % reduction in error when using a modified Dai (2008) landscape classification method for assigned T_A.

For the T_A, T_D, and T_W analysis, dew point temperatures were calculated using Equation (1), a common formula:

$$TD = \left(\frac{RH}{100}\right)^{0.125} * (112 + 0.9 * \mathrm{TA}) + 0.1 * \mathrm{TA} - 112 \quad (1)$$

Since atmospheric pressure was not reported at the Swedish stations, T_W was calculated using an empirical formula (Stull 2011) that does not require air pressure:

$$\begin{aligned} TW = {} & TA \operatorname{atan}[0.151977(RH + 8.313659)^{.5}] \\ & + \operatorname{atan}(TA + RH) - \operatorname{atan}(RH - 1.676331) \\ & + 0.00391838(RH)^{1.5} \operatorname{atan}(0.023101RH) - 4.686035 \quad (2) \end{aligned}$$

Table 2 | GIS landscape classification method using a 15 km buffer

Step 1% land	Step 2 elevation range	Step 3 WW vs LW
<10% land	Ocean/water	Ocean (WW and LW)
10% < land <60%		Coast (WW and LW)
60% < land <90%		Fjord (inlet) (WW and LW)
90% < land	0–499 m	Rolling (WW and LW)
	500–999 m	Hill (WW and LW)
	1,000–1,500 m	Mountain (WW and LW)

For all analysis, the % misclassified precipitation (% error) is:

$$\%\ \text{Error} = \frac{\sum P_S > T_{RS} + \sum P_R \le T_{RS}}{P_{\text{Total}}}, \quad (3)$$

where P_S is a snow precipitation event, P_R is a rain precipitation event, and P_{Total} is the total of all rain and snow precipitation events. T_{RS} is the rain snow temperature threshold value that results in the least misclassified precipitation. Precipitation events rather than mass are used in this analysis due to the Norwegian datasets not containing consistently reported precipitation mass values.

Reduction in error is calculated as:

$$\text{Reduction in Error} = 1 - \frac{\%\ \text{Error}}{\%\ \text{Error using country } T_A}, \quad (4)$$

where the % error from country T_A (Table 1) is used as the reference value.

Datasets for precipitation events with surface air temperatures of −3 to 5 °C were built for each country, landscape, and individual weather station to determine T_A, T_D, and T_W values.

RESULTS AND DISCUSSION

The GIS classification method produced a product similar to that of Feiccabrino's (2015) manual classification (Table 3 and Figure 3). The GIS method resulted in an average reduction in error of 2.29% compared to 2.17% from the manual method. The GIS landscape classification performed better than the manual classification for the Swedish stations (2.42 to 1.24% respectively) but resulted in less error reduction for the Norwegian stations (2.14 to 3.33% respectively). When considering the 18 hill and mountain stations in which there was a difference in T_A between the methods, the GIS and manual landscape classifications resulted in similar reductions in error (2.48 to 2.31% respectively). The largest improvement came from reclassification of the manual LW mountain stations having 0.39% average reduction in error compared to 4.70% when reclassified as LW mountain and LW hill stations in the GIS method.

The results in Figure 3 and Table 3 indicate that the proposed GIS method is able to replicate and/or improve the reduction in misclassified precipitation from manual landscape classification. This landscape classification was done to embrace terrain (Minder *et al.* 2011) and ocean effects (Dai 2008) in the lower atmosphere which are ignored when using a global or regional T_A value, while not downscaling to the individual/hill-slope scale.

The GIS landscape classification was used to assess the use of air, wet bulb and dew-point temperatures in predicting thresholds. Comparing T_A, T_W, and T_D (Figure 4), T_D has more misclassified precipitation than T_A and T_W (Table 3) with most stations having increases in error compared to regional/country T_A (Table 1 and Figure 4). Most study stations are near towns and villages in valleys with sub-saturated atmospheric conditions, so it is expected that the microphysical processes acting on hydrometers would be different than that of the saturated upslope mountain environment used by Marks *et al.* (2013) which found T_D to be a better T_{RS} than T_A and T_W. It is difficult to find weather data on mountains or other sparsely populated areas, much less finding stations reporting more than temperature and precipitation (Kane & Stuefer 2015), that is why improving T_A is an important goal. Here, mostly valley stations were used, so this may have to be considered when choosing a T_{RS} for mountains.

T_A and T_W (Figures 4 and 5) have similar misclassified precipitation results with the exception of LW rolling, and WW ocean landscapes where T_A had the same landscape and regional values while T_W resulted in decreased misclassified precipitation at many of those stations. T_W had the least amount of error averaging 10.76% misclassified precipitation compared to 13.60% for T_D and 11.44% for T_A. T_W also has the most consistent landscape T_{RS} values ranging from 0.3 to 0.6 °C (Table 3). There is little error difference between wet-bulb temperature 0.5 °C and landscape T_W (Table 3) (Figures 5 and 6). However, individual station T_W (13.81%) has a much greater reduction in error than landscape T_W (8.26%) (Figure 6). This indicates more improvement is possible. However, individual station thresholds are not practical when looking for a T_{RS} method for a region with varying landscapes.

The landscape T_A values agreed well with Dai (2008). The warmest values were over the ocean and (WW) Norwegian coast (1.8 and 1.7 °C respectively). However, one surprise was the LW hill stations which have a T_A of 1.6 °C. This could be due to down-sloping effects leading to a deeper dry air layer between the cloud and ground. In a dry layer the air could be assumed to warm at between 9.8 and 7.5 °C/km (Fang *et al.* 2013). Depending on the atmospheric conditions, snow could fall through a couple hundred meters of dry air without completely melting (Venne *et al.* 1997). The coolest T_A values were in the lowlands near the shores indicating that the near surface heating of the ocean does not affect surface or lower atmospheric temperatures far inland (Table 3). Interestingly, T_A values for inland and mountains are warmer (1.2 and 1.3 °C with LW hills at 1.6 °C) than WW fjord and LW coastal stations (1.0 and 1.1 °C respectively). T_{RS} value fluctuations for individual stations within hill and mountain landscapes suggest much of the differences occur on the hill-slope scale as local terrain and winds differ greatly compared to lowland flat terrain. In the winter, oceans cause relatively greater lower atmospheric instability than land due to conductive heating at the ground atmosphere interface leading to warmer T_{RS} values over open water (Ólafsson & Haraldsdóttir 2003). Applying the same logic, one would expect snow covered ground to increase lower atmospheric stability due to cooling at the ground atmosphere interface leading to cooler T_{RS} values over snow covered ground. However, Feiccabrino (2015) did not find any notable variation in T_A values for either land with and without snow cover, or ocean stations with varying sea surface temperatures.

Table 3 | North Sea, Norwegian, and Swedish weather station assigned station numbers, manual and GIS landscape classification with T_A, percentage of misclassified precipitation for T_A, % (less) reduction in error compared to country classification % error (Table 1), with similar analysis for T_D and T_W for the GIS landscape classification

Station # (Figure 1)	Manual landscape	Landscape T_A °C	Landscape % error	% Less error	GIS landscape	Landscape T_A °C	Landscape % error	% Less error	Landscape T_D °C	Landscape % error	% Less error	Landscape T_W °C	Landscape % error	% Less error	T_W 0.5 °C % less error	Station T_A °C
Norwegian stations WW																
1	WW OCEAN	1.8	13.04	0.00	WW OCEAN	1.8	13.04	0.00	−0.4	18.48	−41.72	0.5	11.96	8.28	8.28	1.5
2	WW OCEAN	1.8	25.18	0.00	WW OCEAN	1.8	25.18	0.00	−0.4	19.85	21.17	0.5	21.94	12.87	12.87	2.2
3	WW OCEAN	1.8	15.43	0.00	WW OCEAN	1.8	15.43	0.00	−0.4	19.60	−27.03	0.5	16.51	−7.00	−7.00	1.8
4	WW OCEAN	1.8	14.93	0.00	WW OCEAN	1.8	14.93	0.00	−0.4	17.42	−16.68	0.5	13.61	8.84	8.84	1.8
5	WW COAST	1.8	17.30	2.15	WW COAST	1.7	16.92	4.30	−0.5	25.67	−45.19	0.3	17.49	1.07	1.07	1.5
6	WW COAST	1.8	15.64	5.33	WW COAST	1.7	15.75	4.66	−0.5	20.46	−23.85	0.3	15.72	4.84	4.84	1.9
7	WW COAST	1.8	14.95	−5.50	WW OCEAN	1.8	14.95	−5.50	−0.4	11.84	16.44	0.5	11.46	19.12	19.12	1.0
8	WW COAST	1.8	13.19	5.58	WW OCEAN	1.8	13.19	5.58	−0.4	16.28	−16.54	0.5	13.49	3.44	3.44	1.5
9	WW FJORD	1.0	18.27	1.77	WW FJORD	1.0	18.27	1.77	0.3	22.92	−23.23	0.4	17.61	5.32	−0.91	1.6
10	WW FJORD	1.0	9.03	1.10	WW FJORD	1.0	9.03	1.10	0.3	13.00	−42.39	0.4	8.67	5.04	−1.20	1.2
11	WW FJORD	1.0	12.96	2.78	WW FJORD	1.0	12.96	2.78	0.3	18.89	−41.71	0.4	15.00	−12.53	−12.53	0.7
12	WW FJORD	1.0	8.74	−1.63	WW FJORD	1.0	8.74	−1.63	0.3	12.43	−44.53	0.4	10.26	−19.30	−13.37	1.2
13	WW HILL	1.1	12.94	0.00	WW HILL	1.3	13.44	−3.86	0.0	21.31	−64.68	0.4	15.31	−18.32	−24.11	1.1
14	WW HILL	1.1	12.69	0.00	WW HILL	1.3	12.50	1.50	0.0	13.63	−7.41	0.4	10.96	13.63	15.60	1.5
15	WW HILL	1.1	17.26	0.00	WW HILL	1.3	18.37	−6.43	0.0	15.30	11.36	0.4	14.00	18.89	9.91	0.6
16	WW HILL	1.1	11.90	0.00	WW MTN	1.2	12.06	−1.34	−0.3	14.21	−19.41	0.4	10.93	8.15	5.71	1.1
17	WW MTN	1.4	14.71	7.13	WW HILL	1.3	15.03	5.11	0.0	13.10	17.30	0.4	12.38	21.84	20.33	1.7
18	WW MTN	1.4	10.45	3.15	WW HILL	1.3	10.45	3.15	0.0	11.86	−9.92	0.4	9.60	11.03	9.18	1.3
19	WW MTN	1.4	15.06	2.78	WW MTN	1.2	15.15	2.19	−0.3	19.30	−24.60	0.4	16.35	−5.55	0.39	1.4
20	WW MTN	1.4	8.33	28.62	WW MTN	1.2	9.24	20.82	−0.3	15.00	−28.53	0.4	7.58	35.05	20.82	1.4
Swedish stations LW																
21	LW MTN	1.5	7.20	1.10	LW HILL	1.6	7.25	0.41	0.2	8.47	−16.35	0.5	7.04	3.30	3.30	1.4
22	LW MTN	1.5	16.98	−11.34	LW HILL	1.6	18.20	−19.34	0.2	16.64	−9.11	0.5	14.21	6.82	6.82	0.9
23	LW MTN	1.5	7.04	14.67	LW HILL	1.6	6.70	18.79	0.2	10.05	−21.82	0.5	7.11	13.82	13.82	1.6
24	LW MTN	1.5	8.41	12.12	LW HILL	1.6	8.23	14.00	0.2	10.86	−13.48	0.5	6.48	32.29	32.29	1.7
25	LW MTN	1.5	12.47	−14.61	LW MTN	1.0	9.83	9.65	No RH reported							1.0
26	LW HILL	1.2	9.38	3.50	LW ROLLING	1.3	9.72	0.00	0.3	9.27	4.63	0.5	7.53	22.53	22.53	1.2

(*continued*)

Table 3 | continued

Station # (Figure 1)	Manual landscape	Landscape T_A °C	Landscape % error	% Less error	GIS landscape	Landscape T_A °C	Landscape % error	% Less error	Landscape T_D °C	Landscape % error	% Less error	Landscape T_W °C	Landscape % error	% Less error	T_W 0.5 °C % less error	Station T_A °C
27	LW HILL	1.2	8.48	−6.00	LW ROLLING	1.3	8.00	0.00	0.3	10.93	−36.63	0.5	8.65	−8.12	−8.12	1.4
28	LW HILL	1.2	7.37	−4.39	LW ROLLING	1.3	7.06	0.00	0.3	10.13	−43.48	0.5	6.85	2.97	2.97	1.3
29	LW HILL	1.2	8.65	1.70	LW ROLLING	1.3	8.80	0.00	0.3	9.96	−13.18	0.5	7.45	15.34	15.34	1.1
30	LW HILL	1.2	10.14	3.15	LW ROLLING	1.3	10.47	0.00	0.3	9.98	4.68	0.5	8.62	17.67	17.67	1.0
31	LW ROLLING	1.3	10.85	0.00	LW ROLLING	1.3	10.85	0.00	0.3	12.89	−18.80	0.5	10.13	6.64	6.64	1.3
32	LW ROLLING	1.3	10.97	0.00	LW ROLLING	1.3	10.97	0.00	0.3	12.91	−17.68	0.5	9.97	9.12	9.12	1.5
33	LW ROLLING	1.3	9.04	0.00	LW ROLLING	1.3	9.04	0.00	0.3	8.81	2.54	0.5	7.62	15.71	15.71	1.1
34	LW ROLLING	1.3	6.78	0.00	LW ROLLING	1.3	6.78	0.00	0.3	7.12	−5.01	0.5	5.21	23.16	23.16	1.0
35	LW ROLLING	1.3	8.44	0.00	LW ROLLING	1.3	8.44	0.00	0.3	8.92	−5.69	0.5	7.09	16.00	16.00	1.1
36	LW COAST	1.1	11.37	−1.97	LW COAST	1.1	11.37	−1.97	0.3	13.38	−20.00	0.6	11.52	−3.32	−2.06	1.4
37	LW COAST	1.1	11.51	−5.60	LW COAST	1.1	11.51	−5.60	0.3	12.48	−14.50	0.6	10.83	0.64	−5.50	1.5
38	LW COAST	1.1	11.66	9.26	LW COAST	1.1	11.66	9.26	0.3	13.00	−1.17	0.6	12.18	5.21	4.44	0.8
39	LW COAST	1.1	11.22	2.09	LW COAST	1.1	11.22	2.09	0.3	11.62	−1.40	0.6	10.94	4.54	8.73	1.1
40	LW COAST	1.1	9.54	21.03	LW COAST	1.1	9.54	21.03	0.3	13.31	−10.10	0.6	10.52	12.91	12.91	1.0

Light gray shading indicates stations with a change in T_A between manual and GIS classification.

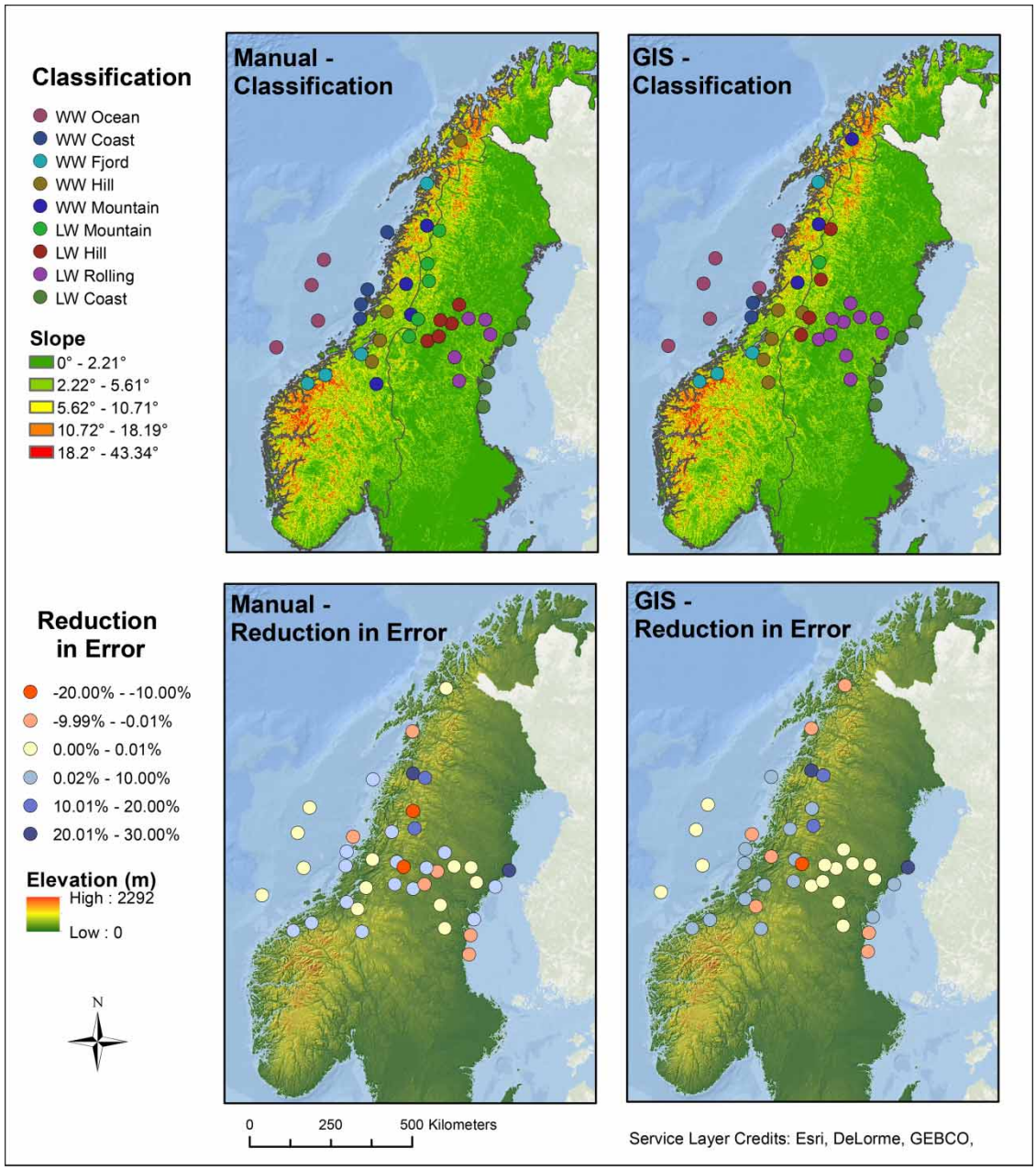

Figure 3 | Top images depict the classification categories on slope/relief maps. The bottom images depict and reduction in error (actual values given in Table 3 under % less error) on a topographic map.

CONCLUSIONS

The GIS landscape classification method was both able to add objectivity to a previous, more subjective, manual classification with similar decreases in misclassified precipitation, indicating that it is a viable method and should be tested in a surface hydrological model.

The GIS landscape T_A results indicate that decreasing the geographical scale from regional/country to sub-regional/landscape reduces misclassified precipitation by 2.29% of the possible 7.60% when using individual station thresholds. The landscapes show ocean stations to have the warmest T_A values while low relief land stations have the coolest. Generally warmer T_A values were found in

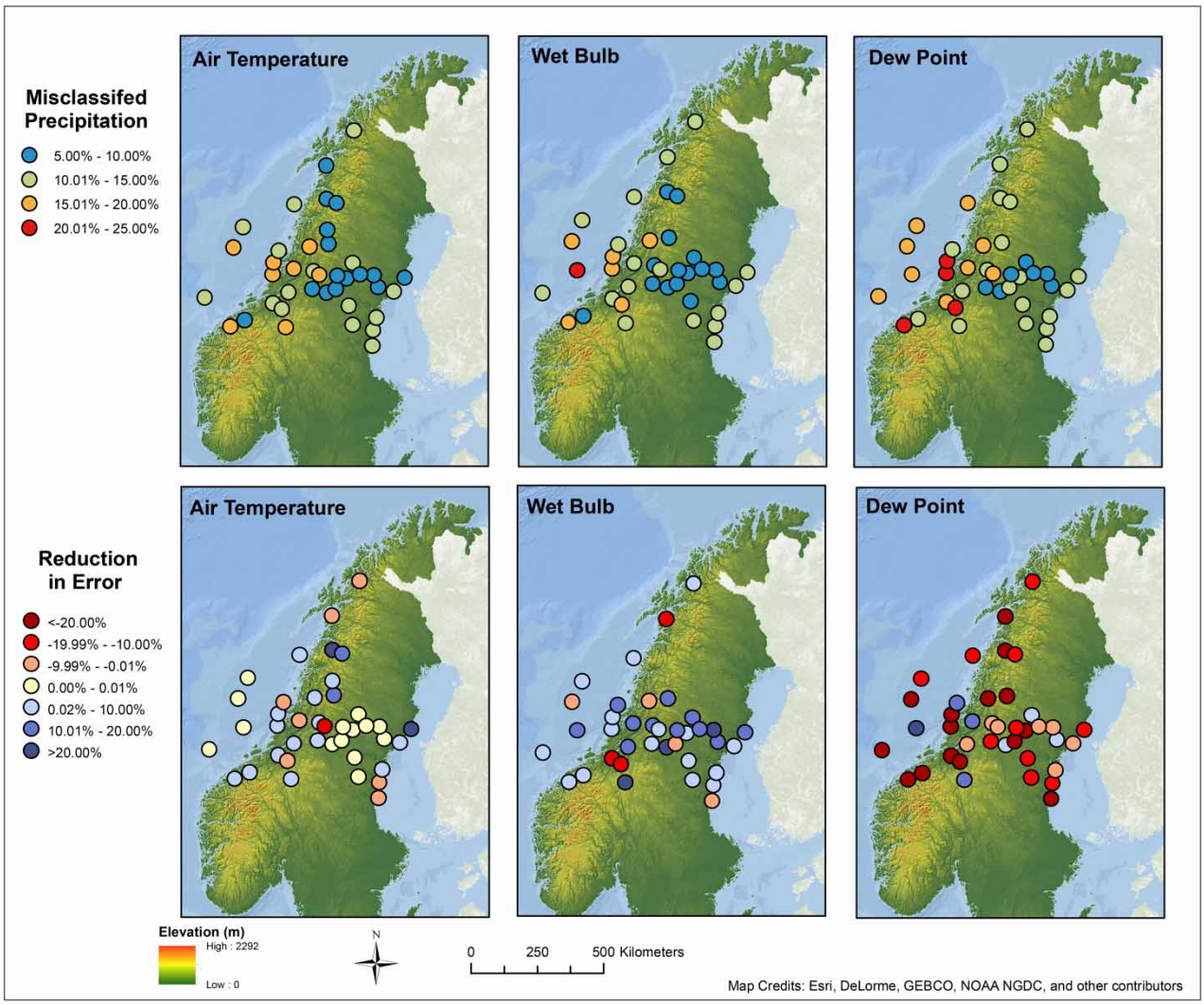

Figure 4 | Misclassified precipitation for GIS landscape T_A, T_W, and T_D values left to right respectively for each station across the top images with their respective reduction in error (actual values given in Table 3 under % less error) in the lower images.

mountain and hill landscapes than for the inland rolling hill or LW coast stations.

Over land, high variability in individual station T_A values were found in mountain and hill landscapes. This indicates that while sub-regional T_A values based on a 15 km GIS landscape identification scheme improved precipitation phase determination, there may be further benefit from a smaller scale GIS analysis modified to identify upslope, downslope, or valley areas within high relief terrain.

Ocean and land effects on T_A were able to advect with prevailing atmospheric winds over coastal stations, most notably for the WW coast and WW ocean landscapes with $T_A = 1.7$ and 1.8 °C respectively and LW rolling, LW coast landscapes with $T_A = 1.3$ and 1.1 °C respectively. The ocean effect did not push further than 15 km inland as fjord/inlet stations had a T_A value of 1.0 °C which is more representative of low relief land stations.

GIS landscape T_W (8.26%) reduced misclassified precipitation from regional T_A by more than three times as much as landscape T_A values (2.29%). Wet-bulb thresholds are superior to T_A for point locations, however many stations do not report the required information to calculate wet-bulb. Therefore, the use of T_W is highly recommended

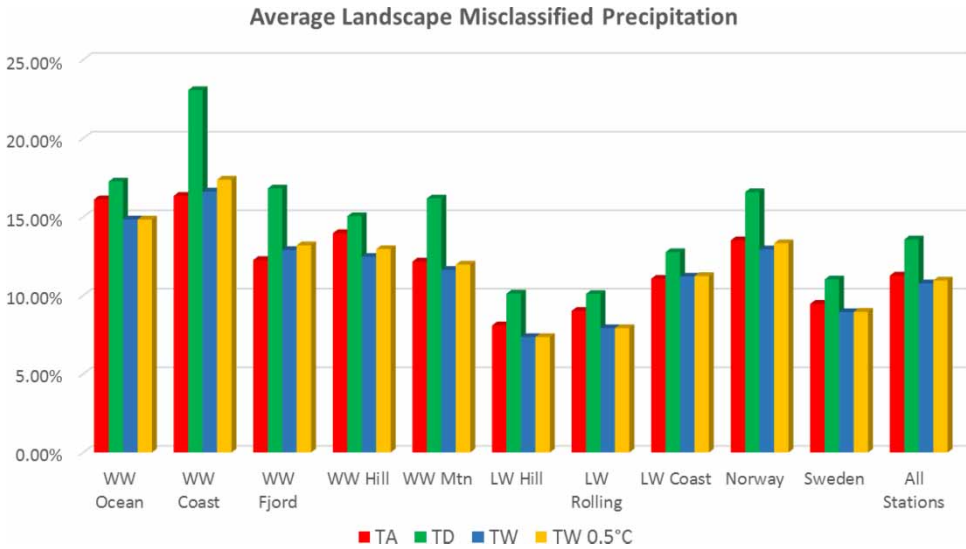

Figure 5 | Average % misclassified precipitation for T_A, T_D, T_W, and $T_W = 0.5\,^{\circ}C$ for stations within each landscape, and average misclassified precipitation using landscape values for the groups of Norwegian (mainland), Swedish, and all stations.

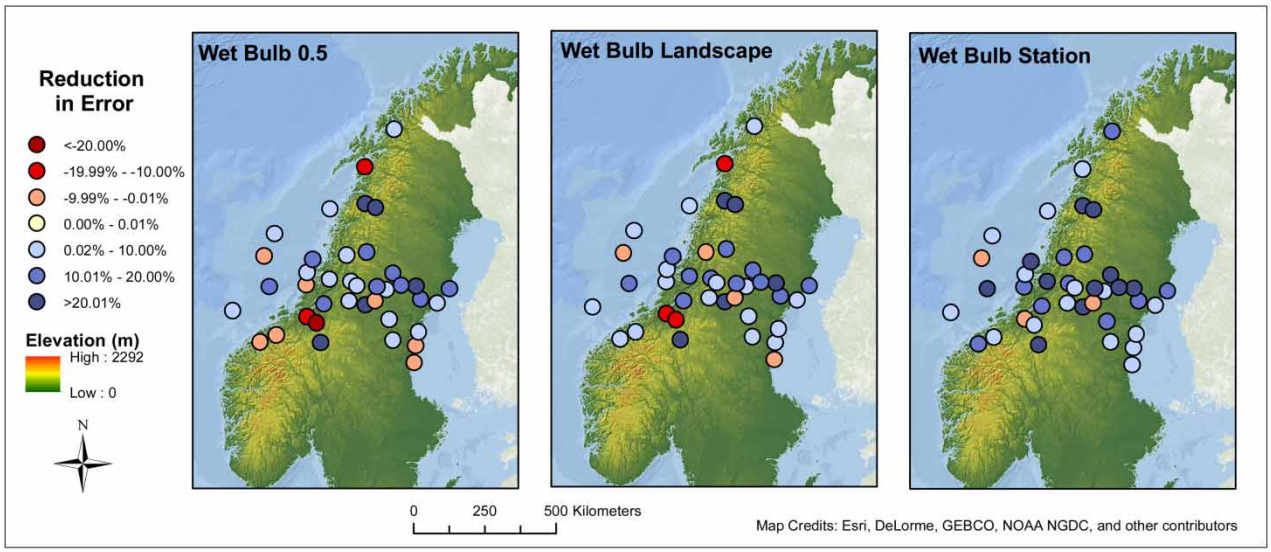

Figure 6 | Comparison of errors (left to right) using $T_W = 0.5\,^{\circ}C$, GIS landscape T_W, and station specific T_W.

if the information exists, or a surface wet-bulb layer is verified to project well through a model layer.

REFERENCES

Dai, A. 2008 Temperature and pressure dependence of the rain-snow phase transition over land and ocean. *Geophys. Res. Lett.* **35** (12), L12802.

Fang, X., Pomeroy, J. W., Ellis, C. R., MacDonald, M. K., DeBeer, C. M. & Brown, T. 2013 Multi-variable evaluation of hydrological model predictions for a headwater basin in the Canadian Rocky Mountains. *Hydrol. Earth Syst. Sci.* **17** (4), 1635–1659.

Feiccabrino, J. 2015 A cross sectional study of rain/snow threshold changes from the North Sea across the Scandinavian Mountains to the Bay of Bothnia. In: *Proceedings of the 20th International Northern Research Basins Symposium and Workshop (20th NRB), Kuusamo, Finland*, 16–21 August, pp. 4–13. Available

from: www.syke.fi/download/noname/%257B8AE2852A-3B60-409A-BE52-574AB5085767%257D/111231 (accessed 23 September 2016).

Feiccabrino, J., Graff, W., Lundberg, A., Sandström, N. & Gustafsson, D. 2015 Meteorological knowledge useful for the improvement of snow rain separation in surface based models. *Hydrology* **2** (4), 266–288.

Harder, P. & Pomeroy, J. 2013 Estimating precipitation phase using a psychrometric energy balance method. *Hydrol. Process.* **27** (13), 1901–1914.

Kane, D. L. & Stuefer, S. 2015 Reflecting on the status of precipitation data collection in Alaska: a case study. *Hydrol. Res.* **46**, 478–493.

Lundberg, A. & Feiccabrino, J. 2009 Sea ice growth, modeling of precipitation phase. In: *Proceedings of the 20th International Conference on Port and Ocean Engineering under Arctic Conditions (POAC 09)*, *Luleå, Sweden*, 9–12 June. Available from: www.poac.com/PapersOnline.html (accessed 23 September 2016), file name POAC09-10.

Marks, D., Winstral, A., Reba, M., Pomeroy, J. & Kumar, M. 2013 An evaluation of methods for determining during-storm precipitation phase and the rain/snow transition elevation at the surface in a mountain basin. *Adv. Water Resour.* **55**, 98–110.

Matsuo, T., Sato, Y. & Sasyo, Y. 1981 Relationship between types of precipitation on the ground and surface meteorological elements. *J. Meteorol. Soc. Jpn.* **59** (4), 462–475.

Minder, J. R., Durran, D. R. & Roe, G. H. 2011 Mesoscale controls on the mountainside snow line. *J. Atmos. Sci.* **68** (9), 2107–2127.

Norwegian Meteorological Institute (NMI) 2016 *Meteorological Data*. Available from: http://eklima.met.no (accessed 30 January 2016).

Ólafsson, H. & Haraldsdóttir, S. H. 2003 Diurnal, seasonal, and geographical variability of air temperature limits of snow and rain. In: *Proceedings of the International Conference on Alpine Meteorology (ICAM 2003)*, *Brig, Switzerland*, 19–23 May, pp. 473–476. Available from: www.map.meteoswiss.ch/map-doc/icam2003/741.pdf (accessed 23 September 2016).

Stenseth, N. C., Mysterud, A., Ottersen, G., Hurrell, J. W., Chan, K. S. & Lima, M. 2002 Ecological effects of climate change. *Science* **5585** (297), 1292–1296.

Stewart, R. E. 1992 Precipitation types in the transition region of winter storms. *Bull. Am. Meteorol. Soc.* **73** (3), 287–296.

Stull, R. 2011 Wet-Bulb temperature from relative humidity and air temperature. *J. Appl. Meteorol. Climatol.* **50**, 2267–2269.

Swedish Meteorological and Hydrological Institute (SMHI) 2016 *Meteorological Data*. Available from: http://opendata-download-metobs.smhi.se/explore/?parameter=8 (accessed 30 January 2016).

Thériault, J. M. & Stewart, R. E. 2010 A parameterization of the microphysical processes forming many types of winter precipitation. *J. Atmos. Sci.* **67** (5), 1492–1508.

United States Army Corps of Engineers (USACE) 1956 *Snow Hydrology*. Summary report of the snow investigations. North Pacific Division, Portland, OR, p. 437.

United States Geological Survey (USGS) 1996 *Global 30 Arc-Second Elevation (GTOP30)*. Available from: https://lta.cr.usgs.gov/GTOPO30.

Venne, M. G., Jasperson, W. H. & Venne, D. E. 1997 *Difficult Weather: A Review of Thunderstorms, Fog, and Stratus, and Winter Precipitation Forecasting*; *AIRFM Command Tech. Report #A246633*, Augsburg Coll Minneapolis MN Center for Atmospheric and Space Sciences, Minneapolis, MN, USA.

First received 31 January 2016; accepted in revised form 17 August 2016. Available online 24 October 2016